# Saturation of the electric field transmitted to the magnetosphere

Wladislaw Lyatsky,[1] George V. Khazanov,[1] and James A. Slavin[1]

Received 10 November 2009; revised 5 April 2010; accepted 16 April 2010; published 20 August 2010.

[1] We reexamined the processes leading to saturation of the electric field, transmitted into the Earth's ionosphere from the solar wind, incorporating features of the coupled system previously ignored. We took into account that the electric field is transmitted into the ionosphere through a region of open field lines, and that the ionospheric conductivity in the polar cap and auroral zone may be different. Penetration of the electric field into the magnetosphere is linked with the generation of the Alfven wave, going out from the ionosphere into the solar wind and being coupled with the field-aligned currents at the boundary of the open field limes. The electric field of the outgoing Alfven wave reduces the original electric field and provides the saturation effect in the electric field and currents during strong geomagnetic disturbances, associated with increasing ionospheric conductivity. The electric field and field-aligned currents of this Alfven wave are dependent on the ionospheric and solar wind parameters and may significantly affect the electric field and field-aligned currents, generated in the polar ionosphere. Estimating the magnitude of the saturation effect in the electric field and field-aligned currents allows us to improve the correlation between solar wind parameters and resulting disturbances in the Earth's magnetosphere.

**Citation:** Lyatsky, W., G. V. Khazanov, and J. A. Slavin (2010), Saturation of the electric field transmitted to the magnetosphere, *J. Geophys. Res.*, *115*, A08221, doi:10.1029/2009JA015091.

## 1. Introduction

[2] Saturation of geomagnetic activity indices, electric field, and cross-polar cap potential transmitted into the magnetosphere during strong geomagnetic activity is a well-known phenomenon that has been widely described in the literature [e.g., *Hill et al.*, 1976; *Weimer et al.*, 1990; *Shepherd et al.*, 2002; *Liemohn et al.*, 2002; *Nagatsuma*, 2002, 2004; *Siscoe et al.*, 2002a, 2002b; *Hairston et al.*, 2003; *Siscoe et al.*, 2004; *Ridley*, 2005; *Shepherd*, 2007; *Lyatsky et al.*, 2007; *Lyatsky and Khazanov*, 2008; *Koustov et al.*, 2009, and references therein]. This effect is of significant interest because of its relevance to Space Weather. However, there is not yet consensus on the mechanism that leads to saturation.

[3] *Siscoe et al.* [2004] and *Ridley* [2005] discussed the different mechanisms proposed for the saturation of the transpolar potential, such as a possible limitation of the reconnection rate near the stagnation point, the effect of processes at the bow shock that can inhibit solar wind plasma from making contacting with the Earth's magnetosphere, and a distortion of the magnetopause that modifies the solar wind flow around the magnetosphere. Unfortunately, due to complexity of the problem, most of the explanations proposed are qualitative.

[4] Recently, *Kivelson and Ridley* [2008] proposed another mechanism to explain the saturation of the electric field and cross-polar potential, transmitted into the magnetosphere. Their principal idea is that the electric field, propagating from the solar wind into the ionosphere as an Alfven wave, is partially reflected when the impedance in the solar wind (which is related to the Alfven wave conductance $\Sigma_A$ and is inversely proportional to the solar wind magnetic field) differs from the impedance of the ionosphere. The reflection may lead to the saturation of the electric field transmitted from the solar wind to the ionosphere. The achievement of this approach is its potential to develop a mathematical model to estimate the electric field transmitted into the magnetosphere without ad hoc assumptions.

[5] For deriving the electric field transmitted to the ionosphere, *Kivelson and Ridley* [2008] used the reflection coefficient for the Alfven wave [e.g., *Scholer*, 1970; *Maltsev et al.*, 1974],

$$E_r = -E_i(\Sigma_P - \Sigma_A)/(\Sigma_P + \Sigma_A), \quad (1)$$

where $E_r$ and $E_i$ are the electric fields of the reflected and incident Alfven waves, respectively, $\Sigma_P$ is the height-integrated Pedersen ionospheric conductance, and

$$\Sigma_A = 1/(\mu_o V_A) \quad (2)$$

is the Alfvén conductance of the solar wind, where $V_A$ is the Alfven velocity. After deriving the electric field of the reflected Alfven wave from (1), *Kivelson and Ridley* [2008] found the transmitted electric field $E_1$ as the sum

[1]NASA Goddard Space Flight Center, Greenbelt, Maryland, USA.

Copyright 2010 by the American Geophysical Union.
0148-0227/10/2009JA015091

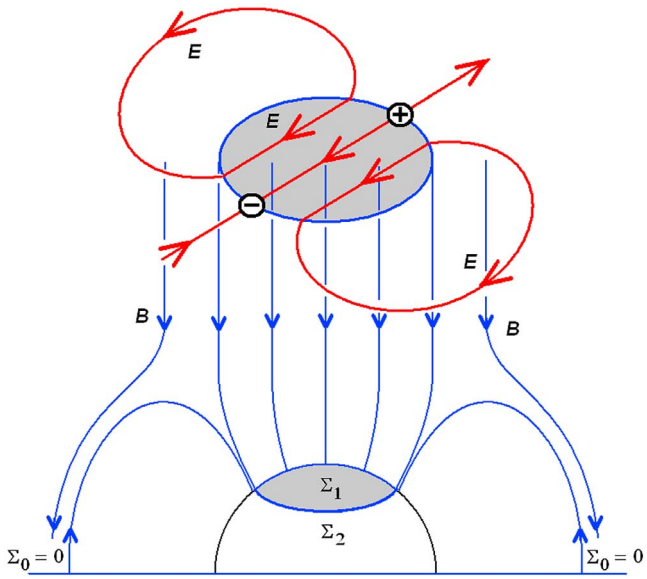


**Figure 1.** A sketch showing the Alfven wave generated in the region of the open field lines over the polar cap. The red curves with arrows show the electric field of this wave inside and outside the region of the open magnetic field lines, shown by the gray circles. Magnetic field lines are shown by the blue lines with arrows.

of the incident ($E_i$) and reflected ($E_r$) electric fields, and (by ignoring convergence of field lines) they obtained the following simple formula for the transmitted electric field

$$E_1 = E_i + E_r = 2E_i\Sigma_A/(\Sigma_P + \Sigma_A). \quad (3)$$

As seen from (3), when $\Sigma_P = \Sigma_A$ there is no reflection and $E_1 = E_i$, i.e., solar wind electric field is totally transmitted into the magnetosphere. The analysis of (3) also shows that with increasing the Alfven conductance of the solar wind, which is inversely proportional to the magnitude of the interplanetary magnetic field (IMF), the transmitted field first increases but when $\Sigma_A$ becomes higher than $\Sigma_P$, the increase in $E_1$ is stopped and the transmitted electric field saturates at $2E_i$.

[6] A similar explanation for the saturation effect earlier was proposed by *Rezhenov* [1983, 1988], who used the results by *Lyatsky and Maltsev* [1983]. While investigating the Alfven wave generated by a conductive disc, moving through magnetized plasma, *Maltsev et al.* [1974] and *Lyatsky and Maltsev* [1983] found the electric field and currents of this Alfven wave. By using their result, *Rezhenov* [1987, 1988] estimated the electric field transmitted from the solar wind to the magnetosphere. He also found that this transmitted electric field should be inversely proportional to the magnitude $\Sigma_P/\Sigma_A$ and concluded that the transmitted electric field "tends to saturate with increasing magnitude of the solar wind magnetic field $B$. The saturation effect is inversely proportional to the solar wind plasma density." But since these works were written originally in Russian, they are generally unfamiliar to the English readers.

[7] The expression (1) in the work of *Kivelson and Ridley* [2008] is related to a simple case when a plane wave is incident on a homogeneous layer. In fact, however, the wave is not plane and the ionospheric conductance is inhomogeneous: during strong geomagnetic disturbances, when the saturation effect is especially significant, the ionospheric conductance in the auroral zone is much higher than that in the polar cap. An additional important feature is that the electric field enters the magnetosphere through a region of open magnetic field lines with a quasi-circular cross section, which is significantly different from the 1-D model of the plane waves. An additional important feature is that the electric field enters the magnetosphere through a region of open magnetic field lines with the quasi-circular cross section, which is significantly less than the area of a region where there are the electric field and currents of the propagating wave.

[8] Figure 1 shows a schematic picture of the Alfven wave generated in the region of open field lines over the polar cap. The red lines with arrows show the electric field of this wave, generated by electric charges, appearing at the boundary of the open magnetic field lines and transported by field-aligned currents along the magnetic field. The electric field of the Alfven wave exists both inside and outside the region of open field lines.

[9] The purpose of the present paper is to investigate the saturation mechanism in more detail by taking into account the more realistic geometry of the problem and different conductivities in high-latitude ionosphere. We calculated the electric field, transmitted from the solar wind into the polar ionosphere, and field-aligned currents at the boundary of open field lines with accounting for the electric field and currents of the Alfven wave, generated over the polar cap and outgoing to the solar wind. We will see that the expressions, obtained for the electric field transmitted into the polar ionosphere, with accounting for the saturation effect may significantly improve the correlation between geomagnetic activity indices and solar wind parameters.

## 2. Method of Solving the Problem

[10] First, we will show that deriving the electric field transmitted into the polar ionosphere may be reduced to solving a simpler problem of deriving the electric field and currents in the model considered earlier by *Maltsev et al.* [1974]. Figure 2 shows the magnetic field and field-aligned currents (FACs) in a meridional cross section of the region of reconnected (open) magnetic field lines. We will consider the problem in the solar-magnetospheric coordinate system. In this coordinate system, the electric field in the free solar wind is $E_0 = -V_{sw} \times B_{sw}$, where $V_{sw}$ is the solar wind speed and $B_{sw}$ is the interplanetary magnetic field. Since this electric field produces in the free solar wind no currents across the magnetic field ($j_\perp = 0$), the conductivity of solar wind plasma across the magnetic field in this coordinate system is zero.

[11] The electric field $E_1$ transmitted into the ionosphere may be different from the ambient solar wind electric field $E_0 = -V_{sw} \times B_{sw}$. On the boundary of the region of open field lines, there are the field-aligned currents $J_\parallel$. These currents are closing through the ionosphere of the polar cap and the auroral zone with the height-integrated conductivities $\Sigma_1$ and $\Sigma_2$, respectively. The inclination of the Alfven wave to the ambient magnetic field (so-called Alfven wings [*Drell*

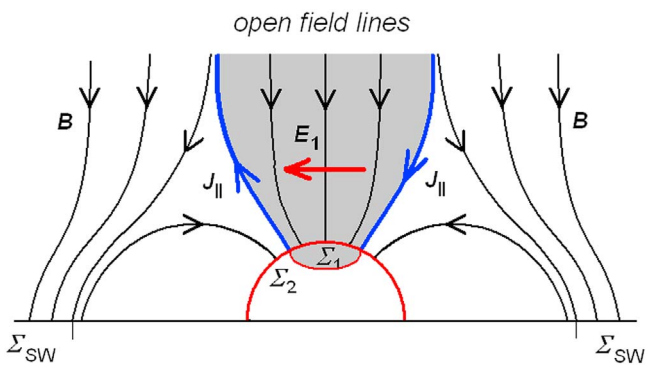


**Figure 2.** A schematic picture of the electric field and *FACs* ($J_{\parallel}$) in the cross section of the region of reconnected (open) magnetic field lines. The black lines with arrows show the magnetic field. The electric field $E_1$ in the region of open field lines is shown with the red arrow. $\Sigma_1$ and $\Sigma_2$ are the ionospheric conductivities in the polar cap and at lower latitudes, respectively, and $\Sigma_{sw}$ is the conductivity of the solar wind across the magnetic field in the region of nonreconnected field lines.

*et al.*, 1965; *Maltsev et al.*, 1977; *Mallinckrodt and Carlson*, 1978]) for simplicity is not considered.

[12] Figure 3 shows schematically the electric field $E_1$ and currents in the cross section of the region of open field lines. The solar wind magnetic field is separated into two regions. One region is related to nonreconnected magnetic field lines going around the magnetosphere, while another region is related to reconnected (open) field lines. In the first region, there is no conductivity across the magnetic field ($\Sigma_{sw} = 0$). In the second region, the reconnected magnetic field lines cross the ionosphere, and on the boundary of this region, there are the field-aligned currents, which are closing through the ionosphere in both polar cap and at lower latitudes.

[13] Let us assume that the polar cap in Figure 3a has the form of a circle with the radius $r_1$ and the Pedersen conductivity $\Sigma_1$. This circle is immersed in the ambient electric field $E_0$. The Pedersen conductivity at lower latitudes (in the auroral zone) is assumed to be $\Sigma_2$. For simplicity, we neglect the Hall ionospheric conductivity and assume that conductivities $\Sigma_1$ and $\Sigma_2$ in each of the regions are uniform that approximately corresponds to the conditions for high geomagnetic activity when the saturation effect is mostly evident. By these conditions, the polarization charges, which appear at the polar cap boundary, create the polarization electric field $E = -\nabla\Phi$ where the electric potential $\Phi$ may be written in the following simple form [see, e.g., *Maltsev et al.*, 1974],

$$\Phi_1 = E_1 r \sin\lambda, \tag{4}$$

$$\Phi_2 = E_1 \left(r_1^2/r\right) \sin\lambda, \tag{5}$$

where indices 1 and 2 are related to the polar cap and the auroral zone, respectively, $E_0$ is the ambient electric field, $r$ is the radius to a point, and $\lambda$ is the polar angle ($\lambda = 0$ corresponds to the meridian where $\Phi_1 = \Phi_2 = 0$). The potentials $\Phi_1$ and $\Phi_2$ are consistent with the Laplace's equation $\nabla^2\Phi = 0$. At the polar cap boundary, $\Phi_1 = \Phi_2 = E_0 r_1 \sin\lambda$.

[14] The radial components $E_r$ of the electric field inside and outside the circle are

$$E_{1r} = -\nabla_r\Phi_1 = -E_1 \sin\lambda, \tag{6}$$

$$E_{2r} = -\nabla_r\Phi_2 = E_1\left(r_1^2/r^2\right) \sin\lambda, \tag{7}$$

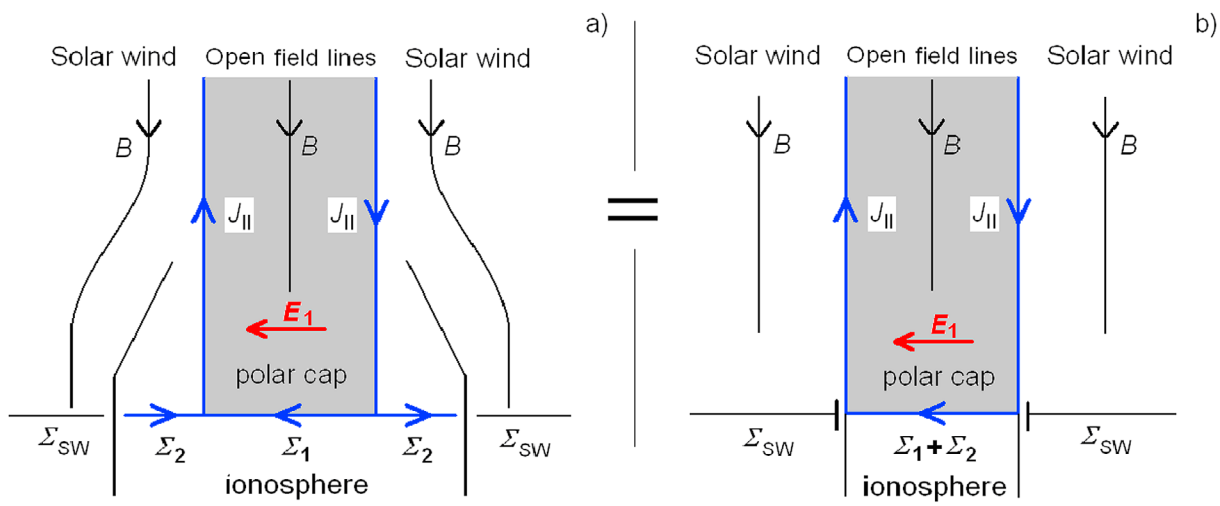


**Figure 3.** (a) Schematic view of the electric field $E_1$, field-aligned currents $J_{\parallel}$, and ionospheric currents in the cross section of the region of reconnected field lines. Black lines with arrows show the magnetic field. The red arrow shows the electric field $E_1$ over the polar cap. $\Sigma_1$ and $\Sigma_2$ are the ionospheric conductivities in the polar cap and at lower latitudes, respectively. $\Sigma_{sw}$ is the conductivity of the solar wind across the magnetic field. (b) The equivalent model, where the conductivities attached to one level and the conductivity in the polar cap is equal to $\Sigma_1 + \Sigma_2$. This model provides the same field-aligned currents and the electric field $E_1$ in the polar cap as those shown in Figure 3a.

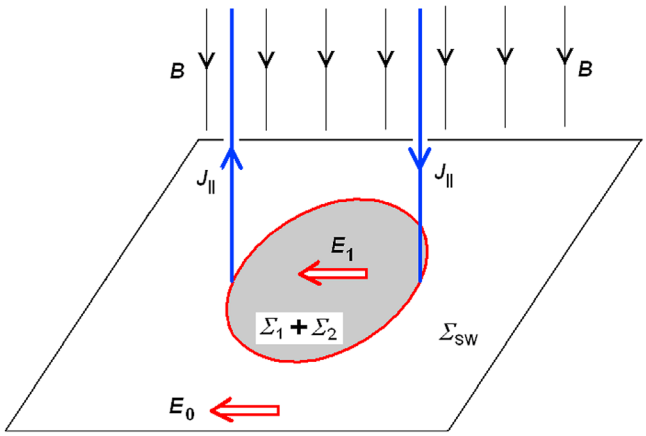


**Figure 4.** The equivalent model for the conductivities, electric field $\boldsymbol{E}_1$ and field-aligned currents $J_{\|}$. The gray area shows the reconnected (open) field lines. The conductivity in the region of open field lines is $\Sigma_1 + \Sigma_2$, while $\Sigma_{sw}$ is the conductivity of the solar wind plasma across the magnetic field. Other designations are the same as shown in Figure 3.

where $E_{r1}$ and $E_{r2}$ are the radial components of the electric field inside and outside the region of open field lines, respectively. These electric fields generate the ionospheric currents, which are closing the field-aligned current at the polar cap boundary,

$$J_{\|} = \Sigma_1 E_{1r} - \Sigma_2 E_{2r}, \tag{8}$$

where $J_{\|}$ is the surface density of the field-aligned current (measured in A/m) and $E_{r1}$ and $E_{r2}$ are the radial components of the electric field in the regions 1 and 2, taken at the polar cap boundary ($r = r_1$). From expressions (6–7), we obtain a simple relation between the radial components of the electric field at the polar cap boundary $E_{1r} = -E_{2r}$. Then the expression (8) for the field-aligned current may be rewritten as follows,

$$J_{\|} = (\Sigma_1 + \Sigma_2)E_{1r}. \tag{9}$$

For the maximum field-aligned current at the polar cap boundary, we obtain the following simple expression,

$$J_{\|}(\max) = (\Sigma_1 + \Sigma_2)E_1, \tag{10}$$

i.e., the field-aligned current $J_{\|}$ on the polar cap boundary is proportional to the sum of the conductivities inside and outside the region. We remind that $J_{\|}$ is the surface density of the field-aligned current (measured in A/m).

[15] Since the field-aligned current $J_{\|}$ is dependent only on the summary conductivity ($\Sigma_1 + \Sigma_2$) in the polar cap and auroral zone, the electric field $E_1$ and field-aligned current remain the same for different $\Sigma_1$ and $\Sigma_2$ if the summary conductivity ($\Sigma_1 + \Sigma_2$) remains the same. This allows us for deriving the electric field and field-aligned currents to use the equivalent model, shown in Figure 3b and in more detail in Figure 4. This equivalent model provides the same electric field in the polar cap and field-aligned currents as those shown in Figures 2 and 3a.

[16] Thus, the problem is reduced to finding the electric field and currents inside and outside the circular region with an effective conductance $\Sigma_{1,\mathrm{eff}} = \Sigma_1 + \Sigma_2$. The outer region in Figure 4 is related to solar wind plasma and the external electric field $E_0 = -V_{sw} \times B_{sw}$. The electric field and conductivities are defined in the coordinate system, immobile with respect to the magnetosphere. The conductivity of solar wind plasma across the magnetic field, by neglecting the collisions, in this approach is equal to zero.

## 3. Solving the Problem and Results Obtained

[17] Thus, by neglecting the convergence of magnetic field lines, the electric field in the polar ionosphere may be found by solving the problem, shown in Figure 4. The problem is reduced to finding the electric field and field-aligned currents over a circular region of an effective conductivity $\Sigma_{\mathrm{eff}} = \Sigma_1 + \Sigma_2$, immersed in the ambient electric field $E_0 = -V_{sw} \times B_{sw}$, generated by the solar wind in the Earth's coordinate frame.

[18] A similar problem had been studied by *Maltsev et al.* [1974]. They found that a circular region of enhanced conductivity, immersed in the ambient magnetic and electric fields, emits the Alfven wave, associated with the field-aligned currents at the boundary of this region and the electric field inside and outside this region, as shown in Figure 1. They obtained the following expression for the electric field $E_1^{\uparrow}$ of the outgoing Alfven wave within this region:

$$E_1^{\uparrow} = -\frac{\Sigma - \Sigma_0}{\Sigma + \Sigma_0^* + 2\Sigma_A} E_0, \tag{11}$$

where $\Sigma$ is the ionospheric conductivity within the circle region, written in the complex form, $\Sigma = \Sigma_P - i\Sigma_H$, where $\Sigma_P$ and $\Sigma_H$ are the Pedersen and Hall conductivities, $\Sigma_0$ is the conductivity outside this circle region, $\Sigma_A$ is the Alfven wave conductivity, $E_0$ are the ambient electric field, and the symbol * means the complex-conjugate quantity.

[19] By neglecting the Hall conductivity and taking into account $E_1^{\uparrow} = E_1 - E_0$, where $E_0$ is the ambient electric field $E_0 = -V_{sw} \times B_{sw}$, we obtain the following expression for the electric field $E_1$ in the polar cap,

$$E_1 = 2\frac{\Sigma_0 + \Sigma_A}{\Sigma + \Sigma_0 + 2\Sigma_A} E_0. \tag{12}$$

To apply this formula to our problem, we should accept $\Sigma_0 = \Sigma_{sw} = 0$ and $\Sigma$ to be equal to the sum of conductivities in the polar cap and auroral zone ($\Sigma = \Sigma_1 + \Sigma_2$), which is accounting for the closure of the field-aligned currents through these two regions. Then we obtain the following expression for the electric field, transmitted from the solar wind into the polar ionosphere,

$$E_1 = \frac{2\Sigma_A}{\Sigma_1 + \Sigma_2 + 2\Sigma_A} E_0. \tag{13}$$

This expression may also be rewritten as follows,

$$E_1 = \frac{1}{1 + (\Sigma_1 + \Sigma_2)/2\Sigma_A} E_0. \tag{14}$$

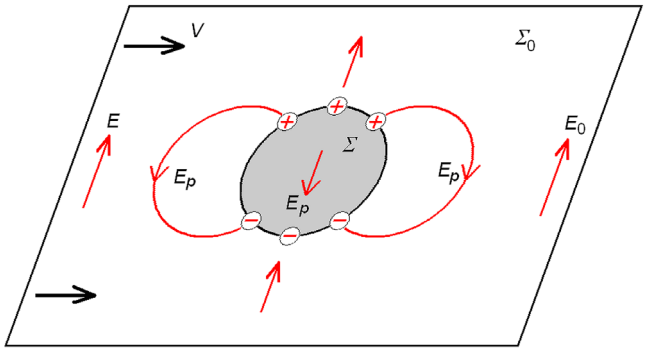


**Figure 5.** Generation of the polarization electric field $E_p$ at the boundary of the circular region of enhanced conductance ($\Sigma > \Sigma_0$).

We note that for the case $\Sigma_1 = \Sigma_2 = \Sigma_A$, the transmitted electric field, given by (13) and (14), is 2 times less than that obtained from (3), and it may be significantly smaller if the conductivities in the polar cap ($\Sigma_1$) and auroral zone ($\Sigma_2$) are different.

[20] Additionally to the expression for the transmitted electric field $E_1$, we may also obtain the expression for the field-aligned currents ($J_\parallel$). The amplitude of the FACs over the ionosphere is

$$J_{\parallel\ \mathrm{ion}} = (\Sigma_1 + \Sigma_2)E_1 = \frac{E_0}{1/(\Sigma_1 + \Sigma_2) + 1/(2\Sigma_A)}. \tag{15}$$

## 4. Discussion

[21] For better understanding the obtained results, we will consider a simple problem, related to generation of the Alfven wave from a region of the enhanced conductance in the ionosphere. Let us assume that in the ionosphere there is a circle with the enhanced conductance $\Sigma$, while the conductance outside this circle is $\Sigma_0$ (Figure 5). There is also an ambient electric field $E_0$ that drives ionospheric plasma at the velocity $V = E \times B/B^2$, where $B$ is the ambient magnetic field directed along the normal to the ionosphere. For simplicity, we will neglect the Hall conductance. The electric charges, appearing at the circle boundary, produce a polarization electric field $E_p$, directed oppositely to the ambient electric field $E_0$.

[22] Figure 5 shows the polarization electric field $E_p$ generated in the ionosphere. This electric field is derived from equations (4) and (5). The total electric field $E_1$ in the polar cap is

$$E_1 = E_0 + E_p. \tag{16}$$

Figure 6 shows the ionospheric currents due to the polarization electric field and field-aligned currents. The left frame shows the currents when the conductivities $\Sigma_1$ and $\Sigma_2$ are not equal to zero. In this case, ionospheric currents $J_p$ flow both inside and outside the circle.

[23] Now let us assume that there are no collisions outside the circle which corresponds to $\Sigma_0 = 0$. In this case, shown on the right frame in Figure 6, there are no ionospheric currents outside the circular region. However, there are the ionospheric currents inside this region, and the summary ionospheric currents $J_1 = \Sigma\ (E_0 - E_p)$ are closing the field-aligned currents $J_\parallel$. This case, related to the flow of collisionless plasma about the conductive circular region, is an exact analogy of the solar wind going about the magnetosphere. Figures 5 and 6 clarify the cause for the saturation effect: the ambient electric field $E_0 = E \times B/B^2$ produces in the conductive body the currents which generate the polarization electric field $E_p$, directed against the ambient electric field $E_0$. As a result, the summary electric field $E_1$ should decrease.

[24] It is instructive to estimate the magnitude of the transmitted electric field $E_1$ by a slightly different way than that considered earlier. Figure 7 shows a sketch of the currents for the case when the ionospheric conductance outside the circle is zero. The total currents inside the circle in Figure 7 are closing the field-aligned currents, which in turn are closing the transverse polarization currents $J_A$ at the front of the outgoing Alfven wave.

[25] The field-aligned currents on the circle boundary may be written as

$$J_\parallel = J_t = \Sigma E_1, \tag{17}$$

where $J_t$ is the total ionospheric currents inside the circle while the field-aligned currents ($J_\parallel$) are closing the polarization currents ($J_A$) generated at the front of the Alfven wave.

[26] The surface density of the transverse polarization currents at the front of the Alfven wave may be written as $J_A = \Sigma_A E_p$ [e.g., *Maltsev et al.*, 1974, 1977; *Mallinckrodt and Carlson*, 1978], where $\Sigma_A$ is the Alfven conductance; this formula has been obtained by integrating the polarization currents of the Alfven wave across its front. For the uniform Alfven conductance, the currents $J_A$ inside and outside the projection of the circle along the field lines provide the equal contributions to the field-aligned current $J_\parallel$. In this case, we obtain $J_\parallel = 2J_A$. Taking also into account $E_p = E_1 - E_0$ yields

$$J_\parallel = 2J_A = -2\Sigma_A(E_1 - E_0). \tag{18}$$

Equaling the expressions (17) and (18) for $J_\parallel$ at the ionosphere level and at the front of the Alfven wave, respectively, yields

$$E_1 = \frac{2\Sigma_A}{\Sigma + 2\Sigma_A}E_0. \tag{19}$$

Returning to the case of the electric field transmitted to the polar cap from the solar wind and assuming $\Sigma$ to be equal to the sum of conductivities in the polar cap and auroral zone (i.e., $\Sigma = \Sigma_1 + \Sigma_2$) for the electric field $E_1$, we obtain from (19) exactly the same expression (14).

### 4.1. Coupling Function

[27] Another important issue, related to the saturation effect, is a chosen solar wind coupling function, which is a combination of solar wind parameters, providing the best fit with geomagnetic indices or the electric field, transmitted

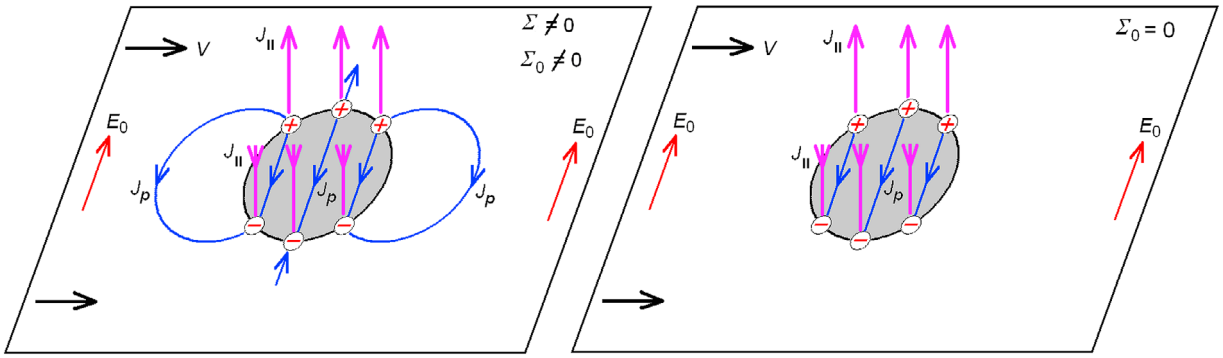


**Figure 6.** Ionospheric polarization currents ($J_p$) and field-aligned currents ($J_{\parallel}$), generated by the polarization electric field, shown in Figure 5. Left frame is related to the case when both $\Sigma$ and $\Sigma_0$ are not equal to zero, while the right frame is related to the case when $\Sigma_0 = 0$.

into the magnetosphere. In this study, we will use the Kan-Lee coupling function [*Kan and Lee*, 1979], which was also used by *Kivelson and Ridley* [2008] for testing their formula for saturation effect. We note that although the Kan-Lee coupling function is not the best among many other coupling functions [e.g., *Akasofu*, 1981; *Lyatsky et al.*, 2007; *Lyatsky and Khazanov*, 2008; *Newell et al.*, 2008, and references therein], this coupling function does not include improving for the saturation effect, which makes convenient using this coupling function for testing a mechanism proposed for improving the saturation effect. We also note that, similar to the Akasofu coupling function [*Akasofu*, 1981], the Kan-Lee coupling function includes the dependence on the clock angle of the IMF (see expression (21)).

[28] Taking into account that the electric field $E_0$, penetrated into the magnetosphere, is derived by a coupling function, the expression (14) for the electric field $E_1$ in the polar cap with accounting for the saturation effect should be rewritten in the form,

$$E_1 = \frac{1}{1 + (\Sigma_1 + \Sigma_2)/2\Sigma_A} F_{K-L}, \tag{20}$$

where the ambient electric field $E_0$ has been replaced with the Kan-Lee coupling function [*Kan and Lee*, 1979], which may be written in the following form,

$$F_{K\text{-}L} \sim V_{sw} B_{yz} \sin^2(\vartheta/2), \tag{21}$$

where $B_{yz}$ is the IMF component in the $y$-$z$ plane in the solar-magnetospheric coordinate system and $\vartheta$ is the angle between the $z$ axis and the IMF vector in the $y$-$z$ plane.

[29] The expression (20) may be rewritten in the form,

$$E_1 = k F_{new}, \tag{22}$$

where $k$ is a coefficient and $F_{new}$ is a new coupling function that is accounting for the saturation effect,

$$F_{new} = \frac{1}{1 + (\Sigma_1 + \Sigma_2)/2\Sigma_A} F_{old}, \tag{23}$$

where $F_{old}$ is an old coupling function (for instance, the Kan-Lee coupling function).

[30] For testing the expressions (22) and (23) and examining how they affect the correlation between magnetic disturbances in the polar cap and solar wind parameters, we used two geomagnetic activity indices: the polar magnetic (PM) index [*Lyatsky and Khazanov*, 2008] and polar cap (PC) index [*Troshichev et al.*, 1988]. Similar to the PC index, the PM index is computed from near-pole geomagnetic observatories, and it shows the magnitude of the equivalent transpolar electrojet, which represents the summary magnetic effect from both ionospheric and field-aligned currents. In distinction from PC index, which measures a component of the transpolar equivalent current in a specific (predominant) direction, the PM index measures this transpolar current even when it significantly differs from its predominant direction. The achievements of PM index also are that it is always positive and shows a significantly better

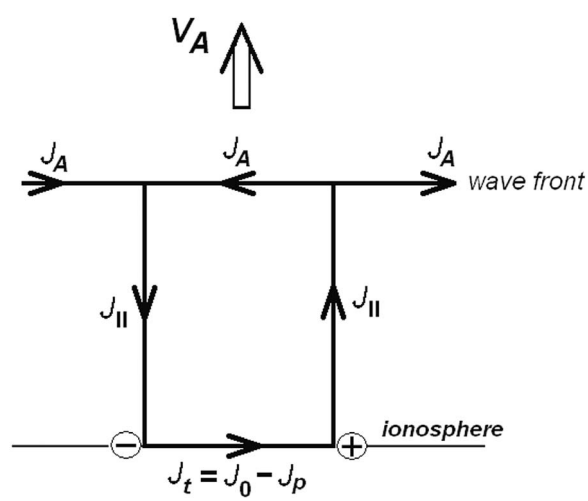


**Figure 7.** A sketch showing the currents related to the outgoing Alfven wave when the conductance outside the circle is zero. $J_t$ is total ionospheric current ($J_t = J_0 - J_p$), $J_0$ is the ionospheric current due to the ambient electric field, $J_p$ is the polarization ionospheric current, $J_{\parallel}$ is the field-aligned current, and $J_A$ are the transverse polarization currents at the front of the outgoing Alfven wave, propagating upward at the Alfven velocity $V_A$.

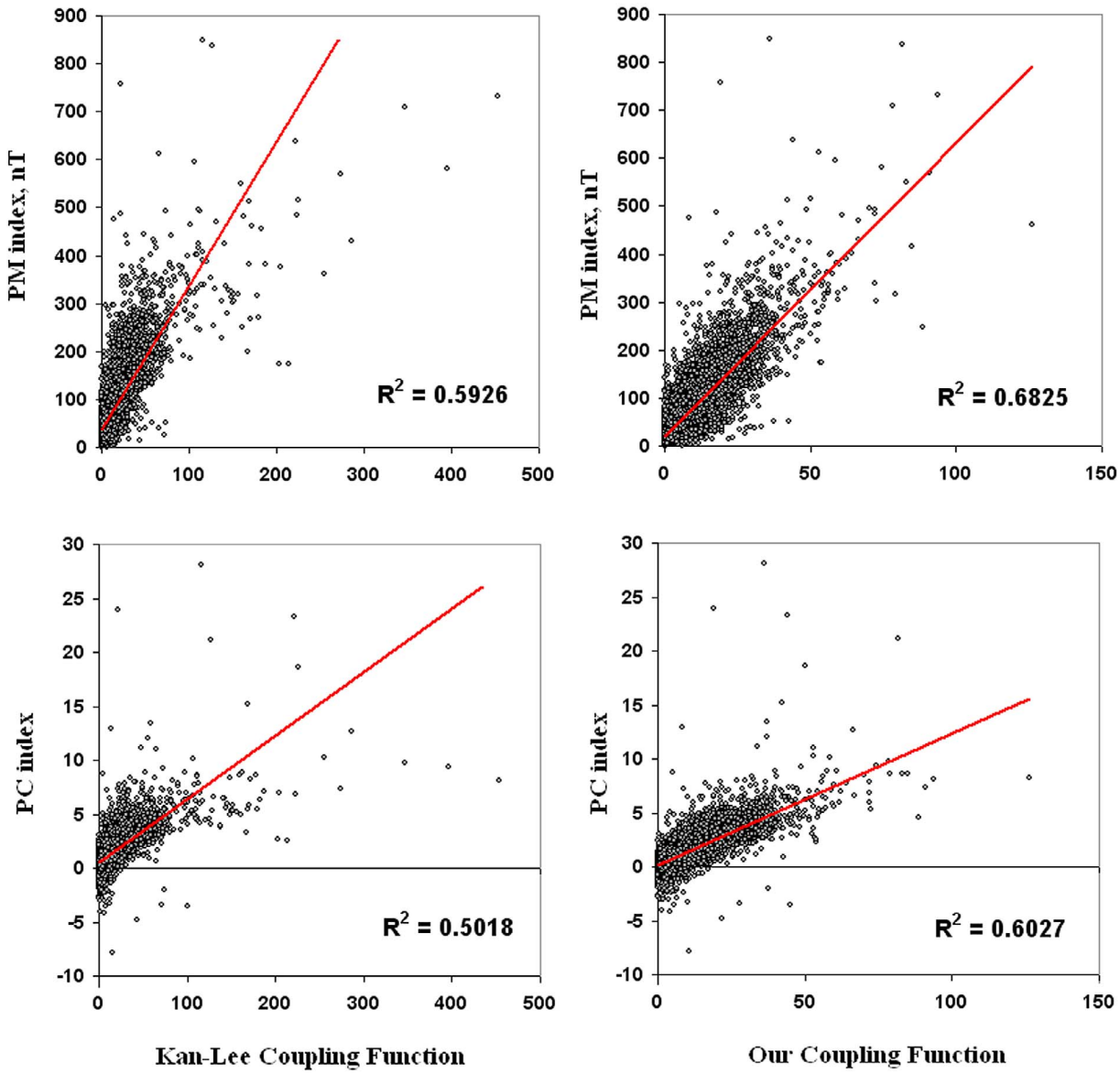


**Figure 8.** Correlation between geomagnetic activity PM and PC indices and (left) the Kan-Lee coupling function and (right) our new coupling function computed for 2 years (2000–2001). Shown are the hourly mean values. The squared correlation coefficients $R^2$ are shown. Each plot includes about 17,520 values. Coupling functions are given in relative units.

correlation than PC index does, with many parameters in the magnetosphere and the solar wind [*Lyatsky and Khazanov*, 2008; *Lyatskaya et al.*, 2008, 2009]. We used, for the analysis, both PM and PC indices for the year 2000 related to solar maximum when there was high enough geomagnetic activity.

[31] Ionospheric conductivities in the polar cap ($\Sigma_1$) and auroral zone ($\Sigma_2$) were estimated as the following. The ionospheric conductance $\Sigma_1$ in the polar cap was assumed to be $\Sigma_1 \approx (1\text{–}3)S$ [e.g., *Hardy et al.*, 1987]. The ionospheric conductivity $\Sigma_2$ in the auroral zone is dependent on geomagnetic activity and was estimated as $\Sigma_2(S) \approx (a + bF^{1/2})$, where $F$ is the Kan-Lee coupling function and the coefficients $a$ and $b$ are 3 and 0.85, respectively.

[32] The Alfven conductivity $\Sigma_A = 1/(\mu_o V_A)$ in the solar wind was estimated as

$$\Sigma_A \approx 30\left[n_{sw}\left(\mathrm{cm}^{-3}\right)\right]^{1/2}/B_{\perp sw}(\mathrm{nT}), \tag{24}$$

where $n_{sw}$ and $B_{sw}$ are the solar wind plasma density and the IMF value. This formula accounts for an approximately 4 times increase in the perpendicular component of the magnetic field and plasma density in the magnetosheath [*Spreiter et al.*, 1966; *Kallio and Koskinen*, 2000] and decreasing in the radial component of the magnetic field near the subsolar point. It also accounts for an increase in the ratio $n^{1/2}/B_{sw}$ in the region of reconnected field lines [e.g., *Samsonov*, 2006] due to annihilation of the magnetic field in reconnection region. This formula is accounting for chang-

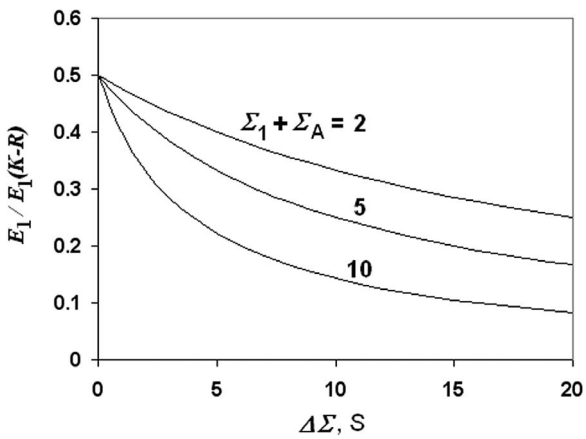


**Figure 9.** The ratio of the electric field $E_1$ transported into the polar ionosphere from our model to that as obtained from the model of the plane waves by *Kivelson and Ridley* [2008] as a function of the difference $\Delta\Sigma$ between the ionospheric conductivities in the auroral zone and polar cap ($\Delta\Sigma = \Sigma_2 - \Sigma_1$) for three values of ($\Sigma_1 + \Sigma_A$) = 2, 5, and 10 S.

ing the Alfven velocity in the region of open field lines though using parameters in the free solar wind does not change significantly the results.

[33] Figure 8 shows an example of the saturation effect in PM and PC indices. On the left frames, shown are the correlation of PM and PC indices with the Kan-Lee coupling function [*Kan and Lee*, 1979] while the two right frames show the correlation of PM and PC indices with the new coupling function (23), which accounts for the saturation effect. One can see that a significant saturation effect on the left frames in Figure 8 is totally reduced on the right frames. Figure 8 also shows that the new coupling function (23) improves significantly the correlation between these two indices and solar wind parameters.

[34] Figure 8 shows that the significant saturation effect on the left frames is totally reduced on the right frames. Thus, Figure 8 shows that using the expressions (22, 23) for the expected electric field in the polar cap strongly reduces the saturation effect and leads to a significant increase in the correlation coefficient for both PM and PC indices. A similar strong increase in the correlation with solar wind parameters is observed in other indices as well (see Figure 11).

### 4.2. Comparison With the Kivelson-Ridley Plane Wave Model

[35] To compare the electric fields in the polar ionosphere, computed from our model and the model of the plane waves by *Kivelson and Ridley* [2008], we calculated from (3) and (14) the ratio $\xi$ of the electric field $E_1$ from our model to the electric field $E_1$(K-R) from Kivelson-Ridley model,

$$\xi = E_1/E_1(\text{K-R}) = \frac{1}{2 + \dfrac{\Delta\Sigma}{\Sigma_1 + \Sigma_A}}, \tag{25}$$

where $\Delta\Sigma = (\Sigma_2 - \Sigma_1)$ is the difference between the conductivities in the auroral zone and polar cap. For $\Delta\Sigma = 0$, the ratio $\xi$ is equal to 0.5; for $\Delta\Sigma > 0$, the ratio $\xi$ is dependent on the quantity $\Delta\Sigma/(\Sigma_1 + \Sigma_A)$.

[36] Figure 9 shows the dependence of the ratio $\xi$ on $\Delta\Sigma$ for three possible values of ($\Sigma_1 + \Sigma_A$).

[37] Figure 9 shows that the electric field $E_1$, transported to the polar ionosphere, in our model may be significantly smaller than that computed from the model of the plane wave by *Kivelson and Ridley* [2008], which for specific situation in the solar wind parameters allows us to explain the strong saturation effect.

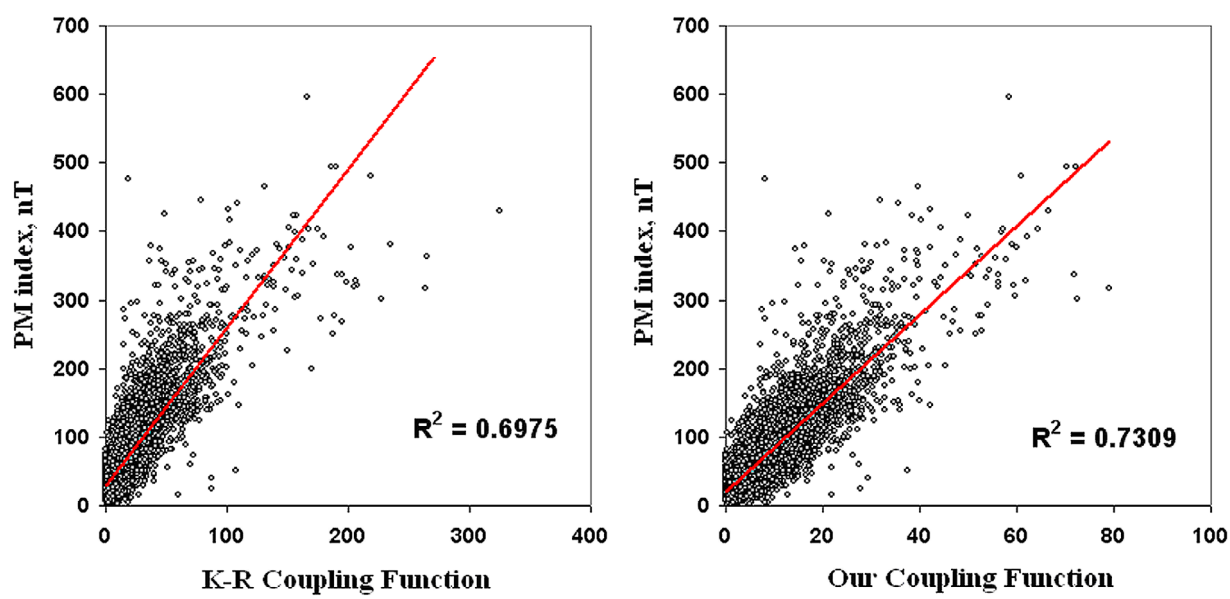


**Figure 10.** Correlation between PM indices and two coupling functions: (left) the Kivelson-Ridley (K-R) coupling function and (right) our new coupling function for the equinoctial months of 2 years (2000–2001). The squared correlation coefficients $R^2$ are shown. Each plot includes about 8760 values. Coupling functions are given in relative units.

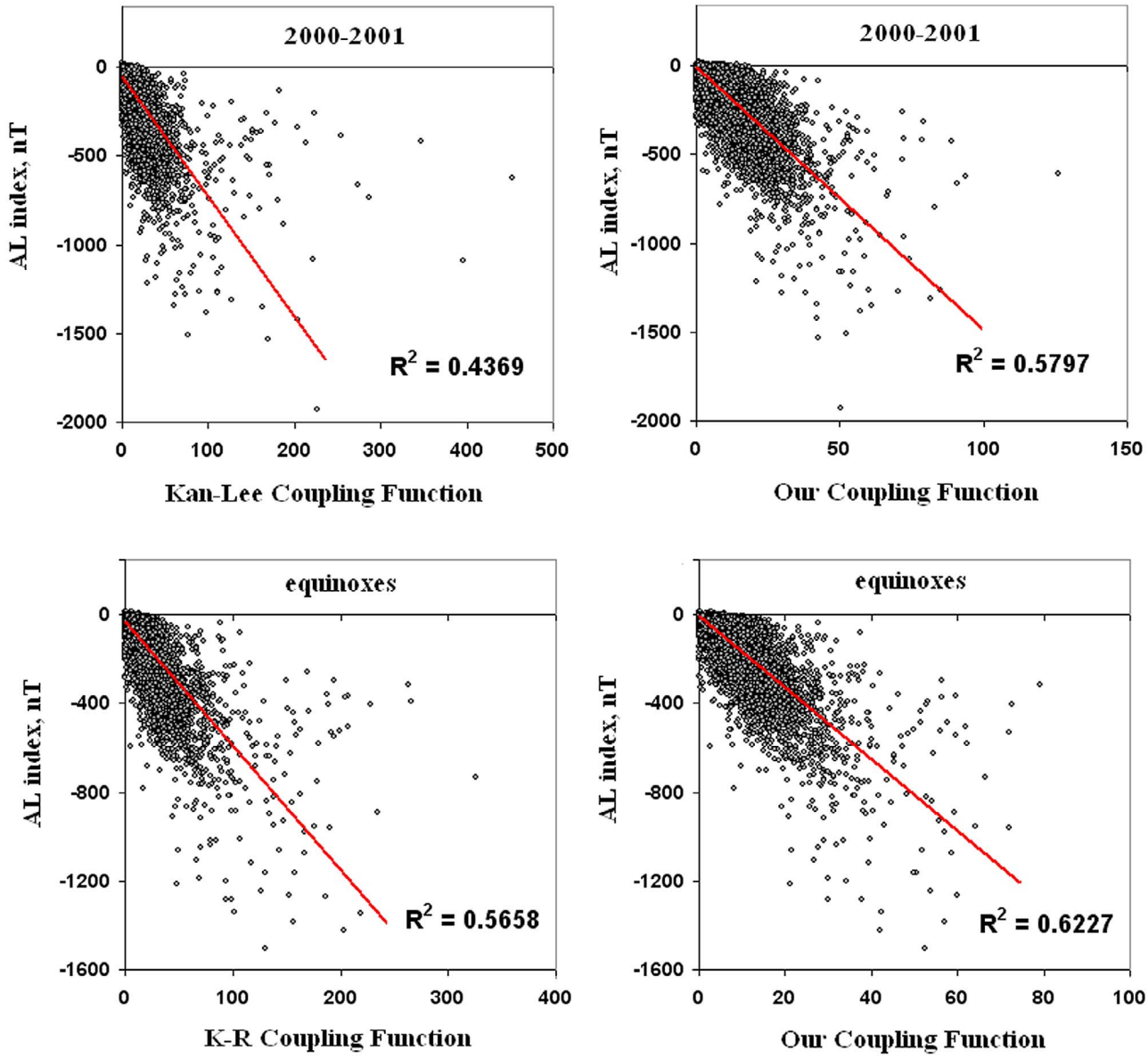


**Figure 11.** (top) Correlation between AL index and (left) the Kan-Lee coupling function and (right) our new coupling function for 2 years (2000–2001). (bottom) Correlation between AL index and (left) the Kivelson-Ridley (K-R) coupling function and (right) our new coupling function for the equinoctial months of the same years (2000–2001). The squared correlation coefficients $R^2$ are shown. Each plot includes about 8760 values. Coupling functions are given in relative units.

[38] Figure 10 shows the correlation plots between PM indices and two coupling functions: the Kivelson-Ridley (K-R) coupling function (on the left) and our new coupling function (on the right). To reduce a significant seasonal variation, we provided here the data only for the six equinoctial months. A similar result shows also the PC index (not shown).

[39] Figure 11 shows the similar correlation plots for another, auroral electrojet (AL) index. Two upper plots show the correlation between AL index and the Kan-Lee coupling function (on the left) and our new coupling function (on the right). Two lower plots show the correlation between AL index and the Kivelson-Ridley coupling function (on the left) and our new coupling function (on the right). To reduce a significant seasonal variation, similar to Figure 10, for two lower plots, we used the data for the six equinoctial months only. To summarize, Figures 10 and 11 show that our model strongly reduces the saturation effect in geomagnetic activity indices when compared with the Kan-Lee coupling function and has a slightly better linear correlation than the Kivelson-Ridley coupling function.

## 5. Summary

[40] Similar to *Rezhenov* [1987] and *Kivelson and Ridley* [2008], the mechanism proposed in this work is based on the idea that the cause for the saturation effect in geomagnetic

activity and the electric field in the polar ionosphere is that the impedance of solar wind plasma on open cap field lines may be inconsistent with the impedance of the ionosphere. However, we solved this problem in a more relevant model of the Alfven wave with the uniform electric field within the polar cap and dipole-like electric field outside it. This wave is propagating into the magnetosphere along the region of open field lines with a quasi-circular cross section and reflected from a nonuniform ionosphere.

[41] The main results of this paper may be summarized as the following. We reexamined the processes leading to saturation of the electric field transmitted into the Earth's ionosphere from the solar wind. We took into account that the electric field is transmitted into the ionosphere through a quasi-circular region of open field lines and that the ionospheric conductivities in the polar cap and auroral zone may be different. Penetration of the electric field into the magnetosphere is linked with the generation of the Alfven wave, going out from the ionosphere into the solar wind and being coupled with the field-aligned currents at the boundary of the open field lines. The electric field of the outgoing Alfven wave reduces the original electric field and provides the saturation effect in the electric field and currents during strong geomagnetic disturbances. The electric field and field-aligned currents of this Alfven wave are dependent on the ionospheric and solar wind parameters and may significantly affect the electric field and field-aligned currents, generated in the polar ionosphere. Estimating the magnitude of the saturation effect in the transmitted electric field and field-aligned currents allows us to improve the correlation between solar wind parameters and resulting disturbances in the Earth's magnetosphere. This mechanism for saturation of the electric field during strong disturbances does not exclude other mechanisms proposed earlier but is important complementary to them.

[42] **Acknowledgments.** We thank Margaret Kivelson for many comments and discussion. This research was performed while Wladislaw Lyatsky held a NASA Senior Postdoctoral Program appointment at NASA/GSFC.

[43] Masaki Fujimoto thanks the reviewers for their assistance in evaluating this paper.

## References

Akasofu, S.-I. (1981), Energy coupling between the solar wind and the magnetosphere, *Space Sci. Rev.*, *28*, 121–190.

Drell, S. D., H. M. Foley, and M. A. Ruderman (1965), Drag and propulsion of large satellites in the ionosphere: An Alfven propulsion engine in space, *J. Geophys. Res.*, *70*, 3131–3146, doi:10.1029/JZ070i013p03131.

Hairston, M. R., T. W. Hill, and R. A. Heelis (2003), Observed saturation of the ionospheric polar cap potential during the 31 March 2001 storm, *Geophys. Res. Lett.*, *30*(6), 1325, doi:10.1029/2002GL015894.

Hardy, D. A., M. S. Gussenhoven, R. Raistrick, and W. J. McNeil (1987), Statistical and functional representations of the patterns of auroral energy flux, number flux, and conductivity, *J. Geophys. Res.*, *92*, 12,275–12,294, doi:10.1029/JA092iA11p12275.

Hill, T. W., A. J. Dessler, and R. A. Wolf (1976), Mercury and Mars: The role of ionospheric conductivity in the acceleration of magnetospheric particles, *Geophys. Res. Lett.*, *3*, 429–432, doi:10.1029/GL003i008p00429.

Kallio, E. J., and H. E. J. Koskinen (2000), A semiempirical magnetosheath model to analyze the solar wind-magnetosphere interaction, *J. Geophys. Res.*, *105*, 27,469–27,479, doi:10.1029/2000JA900086.

Kan, J., and L. Lee (1979), Energy coupling function and solar wind magnetosphere dynamo, *Geophys. Res. Lett.*, *6*, 577–580, doi:10.1029/GL006i007p00577.

Kivelson, M. G., and A. J. Ridley (2008), Saturation of the polar cap potential: Inference from Alfvén wing arguments, *J. Geophys. Res.*, *113*, A05214, doi:10.1029/2007JA012302.

Koustov, A. V., G. Ya. Khachikjan, R. A. Makarevich, and C. Bryant (2009), On the SuperDARN cross polar cap potential saturation effect, *Ann. Geophys.*, *27*, 3755–3764.

Liemohn, M. W., J. U. Kozyra, M. R. Hairston, D. R. Weimer, G. Lu, A. J. Ridley, T. H. Zurbuchen, and R. M. Skoug (2002), Consequences of a saturated convection electric field on the ring current, *Geophys. Res. Lett.*, *29*(9), 1348, doi:10.1029/2001GL014270.

Lyatskaya, S., W. Lyatsky, and G. V. Khazanov (2008), Relationship between substorm activity and magnetic disturbances in two polar caps, *Geophys. Res. Lett.*, *35*, L20104, doi:10.1029/2008GL035187.

Lyatskaya, S., W. Lyatsky, and G. V. Khazanov (2009), Auroral electrojet AL index and polar magnetic disturbances in two hemispheres, *J. Geophys. Res.*, *114*, A06212, doi:10.1029/2009JA014100.

Lyatsky, W., and G. V. Khazanov (2008), A new polar magnetic index of geomagnetic activity, *Space Weather*, *6*, S06002, doi:10.1029/2007SW000382.

Lyatsky, W., S. Lyatskaya, and A. Tan (2007), A coupling function for solar wind effect on geomagnetic activity, *Geophys. Res. Lett.*, *34*, L02107, doi:10.1029/2006GL027666.

Mallinckrodt, A. J., and C. W. Carlson (1978), Relations between transverse electric field and field-aligned currents, *J. Geophys. Res.*, *83*(A4), 1426–1432, doi:10.1029/JA083iA04p01426.

Maltsev, Yu. P., S. V. Leontyev, and W. B. Lyatsky (1974), Pi2 pulsations as a result of evolution of an Alfven impulse originating in the ionosphere during a brightening of aurora, *Planet. Space Sci.*, *22*, 1519–1533.

Maltsev, Yu. P., W. B. Lyatsky, and A. M. Lyatskaya (1977), Currents over the auroral arc, *Planet. Space Sci.*, *25*, 53–57.

Merkin, V. G., A. S. Sharma, K. Papadopoulos, G. Milikh, J. Lyon, and C. Goodrich (2005), Global MHD simulations of the strongly driven magnetosphere: Modeling of the transpolar potential saturation, *J. Geophys. Res.*, *110*, A09203, doi:10.1029/2004JA010993.

Merkine, V. G., K. Papadopoulos, G. Milikh, A. S. Sharma, X. Shao, J. Lyon, and C. Goodrich (2003), Effects of the solar wind electric field and ionospheric conductance on the cross polar cap potential: Results of global MHD modeling, *Geophys. Res. Lett.*, *30*(23), 2180, doi:10.1029/2003GL017903.

Nagatsuma, T. (2002), Saturation of polar cap potential by intense solar wind electric fields, *Geophys. Res. Lett.*, *29*(10), 1422, doi:10.1029/2001GL014202.

Nagatsuma, T. (2004), Conductivity dependence of cross-polar potential saturation, *J. Geophys. Res.*, *109*, A04210, doi:10.1029/2003JA010286.

Newell, P., T. Sotirelis, K. Liou, and F. Rich (2008), Pairs of solar wind-magnetosphere coupling functions: Combining a merging term with a viscous term works best, *J. Geophys. Res.*, *113*, A04218, doi:10.1029/2007JA012825.

Rezhenov, B. V. (1987), The influence of wave conductivity of the solar wind on convection in the polar cap, *Geomagn. Aeron.*, *27*, 532–534.

Rezhenov, B. V. (1988), in *Physics of Auroral Phenomena*, edited by B. E. Brunelli and W. B. Lyatsky, pp. 4–22, Leningrad, "Nauka," 1988 (in Russian).

Ridley, A. J. (2005), A new formulation for the ionospheric cross polar cap potential including saturation effects, *Ann. Geophys.*, *23*, 3533–3548.

Samsonov, A. (2006), Numerical modelling of the Earth's magnetosheath for different IMF orientations, *Adv. Space Res.*, *38*, 1652–1656.

Scholer, M. (1970), On the motion of artificial ion clouds in the magnetosphere, *Planet. Space. Sci.*, *18*, 977–1004.

Shepherd, S. G. (2007), Polar cap potential saturation: Observations, theory, and modeling, *J. Atmos. Sol. Terr. Phys.*, *69*, 234–248, doi:10.1016/j.jastp.2006.07.022.

Shepherd, S. G., R. A. Greenwald, and J. M. Ruohoniemi (2002), Cross polar cap potentials measured with Super Dual Auroral Radar Network during quasi-steady solar wind and interplanetary magnetic field conditions, *J. Geophys. Res.*, *107*(A7), 1094, doi:10.1029/2001JA000152.

Siscoe, G. L., G. M. Erickson, B. U. Ö. Sonnerup, N. C. Maynard, J. A. Schoendorf, K. D. Siebert, D. R. Weimer, W. W. White, and G. R. Wilson (2002a), Hill model of transpolar potential saturation: Comparisons with MHD simulations, *J. Geophys. Res.*, *107*(A6), 1075, doi:10.1029/2001JA000109.

Siscoe, G. L., N. U. Crooker, and K. D. Siebert (2002b), Transpolar potential saturation: Roles of region 1 current system and solar wind ram pressure, *J. Geophys. Res.*, *107*(A10), 1321, doi:10.1029/2001JA009176.

Siscoe, G., J. Raeder, and A. J. Ridley (2004), Transpolar potential saturation models compared, *J. Geophys. Res.*, *109*, A09203, doi:10.1029/2003JA010318.

Spreiter, J. R., A. L. Summers, and A. Y. Alksne (1966), Hydromagnetic flow around the magnetosphere, *Planet. Space. Sci.*, *14*, 223–253.

Troshichev, O. A., V. G. Andrezen, S. Vennerstrom, and E. Friis-Christensen (1988), Magnetic activity in the polar cap – A new index, *Planet. Space Sci.*, *36*, 1095–1102.

Weimer, D. R., L. A. Reinleitner, J. R. Kan, L. Zhu, and S.-I. Akasofu (1990), Saturation of the auroral electrojet current and the polar cap potential, *J. Geophys. Res.*, *95*, 18,981–18,987, doi:10.1029/JA095iA11p18981.

G. V. Khazanov, W. Lyatsky, and J. A. Slavin, NASA Goddard Space Flight Center, Greenbelt, MD 20771, USA. (lyatsky@gmail.com)